

Level-1 pixel based tracking trigger algorithm for LHC upgrade

Chang-Seong Moon* and Aurore Savoy-Navarro

*Laboratoire APC, Université Paris Diderot-Paris7/CNRS,
10, rue Alice Domon et Léonie Duquet 75205 Paris Cedex 13, France
E-mail: csmoon@cern.ch*

ABSTRACT: The Pixel Detector is the innermost detector of the tracking system of the Compact Muon Solenoid (CMS) experiment at CERN Large Hadron Collider (LHC). It precisely determines the interaction point (primary vertex) of the events and the possible secondary vertexes due to heavy flavours (b and c quarks); it is part of the overall tracking system that allows reconstructing the tracks of the charged particles in the events and combined with the magnetic field to measure their impulsion. The pixel detector allows measuring the tracks in the region closest to the interaction point. The Level-1 (real-time) pixel based tracking trigger is a novel trigger system that is currently being studied for the LHC upgrade. An important goal is developing real-time track reconstruction algorithms able to cope with very high rates and high flux of data in a very harsh environment. The pixel detector has an especially crucial role in precisely identifying the primary vertex of the rare physics events from the large pile-up (PU) of events. The goal of adding the pixel information already at the real-time level of the selection is to help reducing the total level-1 trigger rate while keeping an high selection capability. This is quite an innovative and challenging objective for the experiments upgrade for the High Luminosity LHC (HL-LHC). The special case here addressed is the CMS experiment. This document describes exercises focusing on the development of a fast pixel track reconstruction where the pixel track matches with a Level-1 electron object using a ROOT-based simulation framework.

KEYWORDS: HL-LHC; CMS; Pixel tracker; Level-1 trigger; Real-time track reconstruction algorithm.

*Corresponding author, supported by the FP7-PEOPLE-2011-IIF, Contract No. 302103, “TauKitForNewPhysics”.

Contents

1. Introduction	1
2. The upgrade of the Pixel detector from Phase 1 to Phase 2	2
3. The L1 pixel based Electron trigger algorithm	2
3.1 Pattern recognition seeded by the L1 EM cluster	4
3.1.1 Pattern recognition in the $R - \phi$ transverse plane	4
3.1.2 Refined Pattern recognition seeded by the EM cluster	5
3.2 The standalone pattern recognition	6
4. Preliminary outcomes from feasibility studies on a L1 pixel based electron trigger	6
5. EXERCISES	7
6. Conclusion	11

1. Introduction

The LHC experiments ran successfully and provided excellent data at the central collision energy of 7 to 8 TeV. ATLAS and CMS collaborations have discovered in 2012 a new boson with a mass near 125 GeV and properties compatible so far with those predicted for the standard model Higgs boson. The discovery of the Higgs boson completes the set of predicted particles by the Standard Model (SM) of particle physics.

The LHC will start operating at the central collision energy of 13 TeV initially in 2015 and progressively reaching the design energy of 14 TeV. This is a new energy frontier. It will substantially enlarge the mass reach in the search for new particles and will also greatly extend the potential to study the properties of the Higgs boson and to explore the overall Higgs sector. In order to meet the experimental challenges of unprecedented proton-proton luminosity, the CMS collaboration will need to improve and upgrade the ability of the apparatus to isolate and precisely measure the products of the most interesting collisions. Therefore, a key goal of the LHC upgrade will be to maintain the overall physics acceptance under the challenging HL-LHC conditions (140 average PU events up to even 200 PU in average and an instantaneous luminosity of $5 \times 10^{34} \text{ cm}^{-2}\text{s}^{-1}$). CMS must preserve its capability to efficiently trigger events originating from low-mass physics processes (e.g. Higgs production at 125 GeV) and for performing precision measurements of low to medium transverse momentum (p_T) physics objects in particular all the leptons (electrons, muons and taus), the heavy quarks especially the b -quark and consequently the top-quark, as well as distinguishing the photons from the electrons. A series of ongoing feasibility studies are conducted

within the CMS experiment; they show the benefits of having the pixel information included in the Level-1 (L1) track trigger. The next crucial challenge is of course to show the real possibility to include it in a realistic scenario taking into account the constraints in bandwidth and latency at the L1 trigger in the LHC experiments (ATLAS and CMS).

Section 2 are briefly described the CMS pixel detector and its sequential upgrades in Phase 1 and Phase 2. We introduce in Section 3, as an example, a L1 pixel tracking algorithm, called PiXTRK. It is a first attempt to achieve a real-time track reconstruction using the pixel clusters within a region seeded by the L1 electromagnetic (EM) calorimeter trigger tower. Section 4 briefly reports the main results obtained by the feasibility studies on the L1 pixel based trigger potential in CMS. Section 5 describes in more details the exercises given to the students in the international Summer School on "INtelligent Signal Processing for FrontIER Research and Industry" held in Paris [4].

2. The upgrade of the Pixel detector from Phase 1 to Phase 2

The present CMS pixel detector consists of three barrel layers with two endcap disks that covers a pseudorapidity range $|\eta| < 2.5$, matching the acceptance of the central tracker [1]. A first upgrade for Phase 1 (around 2018) of the current pixel detector will consist in adding a fourth barrel layer, a third disk on each endcap sides, as well as a new Front End ASIC including signal digitization, and consequently a new readout chain with higher performance in speed and bandwidth. The main motivation for the Phase 1 upgrade of the pixel detector is to maintain the high efficiencies and low fake rates and to minimize the data loss due to latencies and limited buffering in higher luminosity running conditions [2]. In the Phase 2 upgrade for HL-LHC, the CMS pixel detector will have an extended pseudorapidity coverage up to $|\eta| < 4$ as shown in figure 1 [5]. It will be made of new pixel sensors (the sensor technology is being selected) and of smaller size pixels (higher granularity). A new Front End and readout system is currently developed within the R&D (RD53) Collaboration [6] for the HL-LHC era (2023-2025).

3. The L1 pixel based Electron trigger algorithm

This series of exercises concentrates on the application of the pixel detector to the electron trigger. The PiXTRK algorithm we are using here and that has been developed for ongoing feasibility studies in CMS for HL-LHC, performs the *pattern recognition*. This is the first step for the track reconstruction. To do so, PiXTRK transfers to Level-1 what is actually achieved in the first stage of the CMS High Level Trigger (HLT), namely the matching of pixel hits with the EM cluster [3]. The pattern recognition proceeds by first defining $\Delta\phi$ windows (*i.e.* in the transverse plane to the beam axis), seeded by the EM cluster, and going backward to the beam spot (figure 3). The limit conditions imposed on all signal windows vary as a function of EM E_T . Furthermore PiXTRK distinguishes between positive and negative charged particles, here electrons and positrons. But unlike the HLT case, at Level-1, it is not possible to use hits, because of bandwidth limitation, and thus we consider pixel clusters and it is not possible to benefit of a refined EM cluster calorimeter reconstruction; what is only available here, is the EM cluster as defined at the L1 calorimeter level.

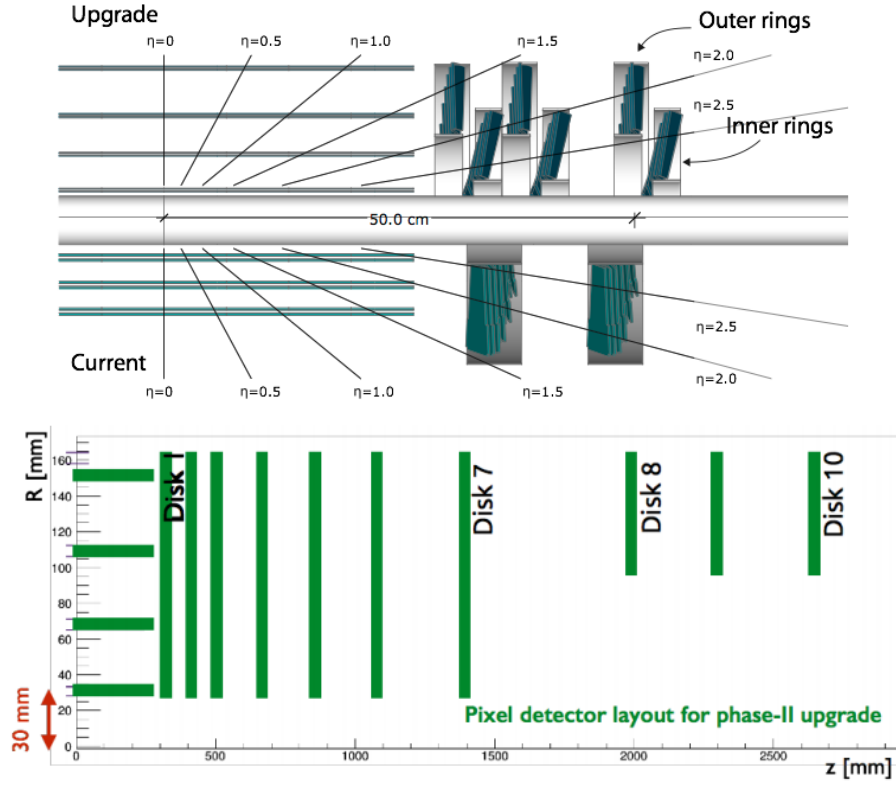


Figure 1. Present and Phase 1 pixel detector layouts (top) and Phase 2 upgrade layout (bottom)

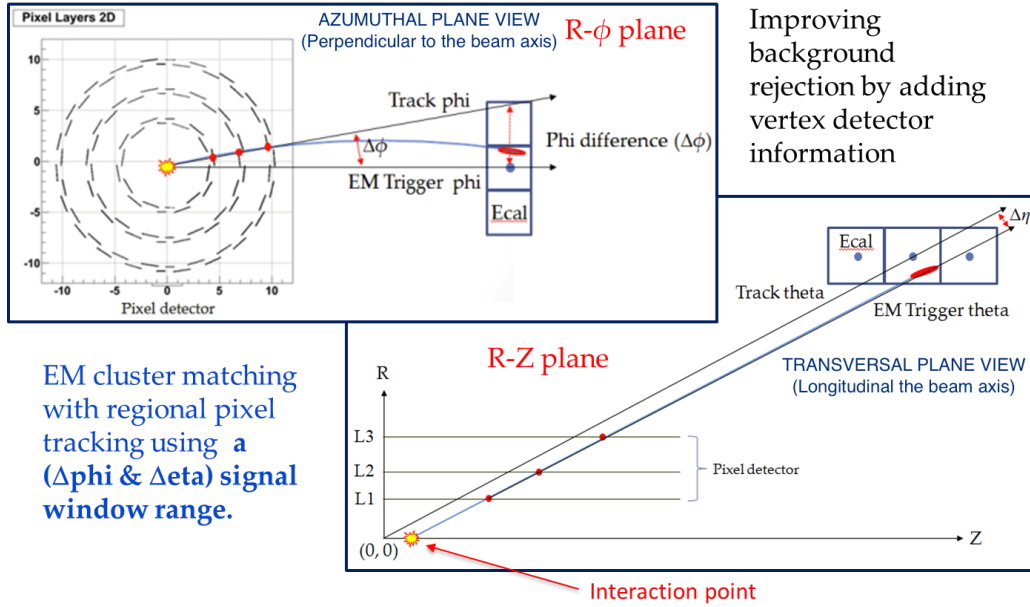


Figure 2. Schema summarizing the PiXTRK pattern recognition strategy in the azimuthal and transversal plane views for the current pixel barrel layout

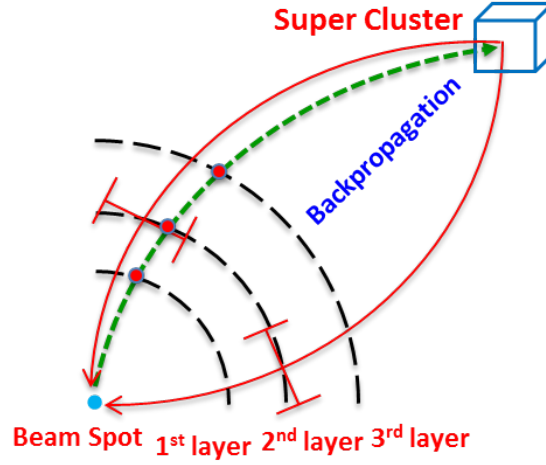


Figure 3. Schema describing the Pixel matching with the Super Cluster in HLT

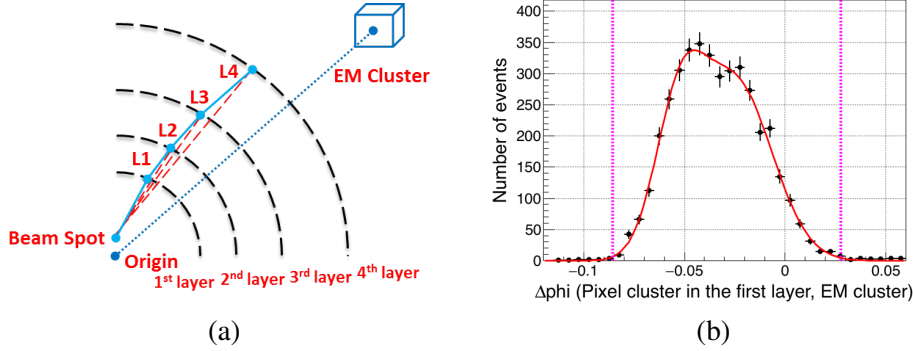


Figure 4. Pixel track matching with EM cluster in $\Delta\phi$: (a) each pixel layer L_i one look to ϕ angle between (BS, L_i) and (BS, EM) , and (b) $\Delta\phi = \phi(BS, L_1) - \phi(BS, EM)$ plot and three sigma boundary.

The pattern recognition proceeds then in 2 stages which are described in a bit more details in subsections 3.1 and 3.2.

3.1 Pattern recognition seeded by the L1 EM cluster

It follows two steps:

3.1.1 Pattern recognition in the $R - \phi$ transverse plane

First is considered the region of interest (RoI) defined, in the transverse $R - \phi$ plane, by the L1 EM cluster linked to the beam spot (BS). In this region are selected the pixel clusters which, in each layer (L_i , $i=1, \dots, 4$) are included in a $\Delta\phi$ window defined here by $\Delta\phi < 0.1$, and considering both the cases of electrons and positrons. The selected pixel clusters in each layer are those which are in the $\Delta\phi$ window (figure 4) defined as:

$$\Delta\phi = \phi(BS, L_i) - \phi(BS, EM) \quad (3.1)$$

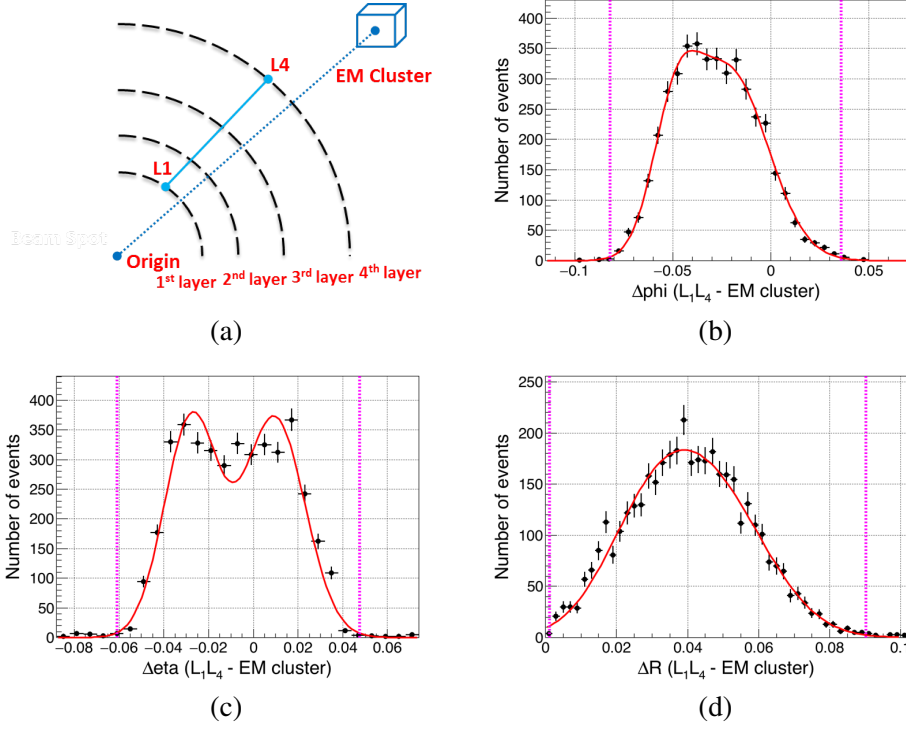


Figure 5. Pixel track matching with EM cluster in $\Delta\eta$, $\Delta\phi$ and ΔR , combining 2 by 2 the pixel layers: here shown the case coupling pixel clusters in L_1 and L_4 layers (a) corresponding (L_1, L_4) segment matching in ϕ with (BS, EM) segment; (b) corresponding $\Delta\phi = \phi(L_1, L_4) - \phi(BS, EM)$ distribution; (c) corresponding $\Delta\eta = \eta(L_1, L_4) - \eta(BS, EM)$ distribution; (d) corresponding $\Delta R = \sqrt{(\Delta\eta)^2 + (\Delta\phi)^2}$; All the distributions include the three sigma boundary and correspond to EM transverse energy (E_T) range from 20 to 21 GeV.

Where (BS, L_i) is the pixel segment joining the beam spot with the relevant pixel cluster in the corresponding L_i layer. The segment of (BS, EM) joins the beam spot with the L1 EM cluster. In the case of more than one cluster satisfying the equation 3.1, all the combinations corresponding to all the possible clusters in this region of interest are considered. The pattern recognition proceeds further on for refining the pattern recognition procedure according to the two following steps.

3.1.2 Refined Pattern recognition seeded by the EM cluster

It consists in determining now the $\Delta\eta$, $\Delta\phi$ and ΔR signal windows, in function of EM E_T , for the set of the pixel clusters selected by the condition defined by the equation 3.1, for each layer. The pixel layers are combined 2 by 2 to form all the possible (L_i, L_j) track segments which correspond to each pixel cluster retained in the selection defined by the condition (3.1). It compares the matching of each of these (L_i, L_j) segments with the segment joining the beam spot with the EM cluster in the (η, ϕ) coordinates by defining:

$$\begin{aligned}\Delta\eta &= \eta(L_i, L_j) - \eta(BS, EM) \\ \Delta\phi &= \phi(L_i, L_j) - \phi(BS, EM) \\ \Delta R &= \sqrt{(\Delta\eta)^2 + (\Delta\phi)^2}\end{aligned}\tag{3.2}$$

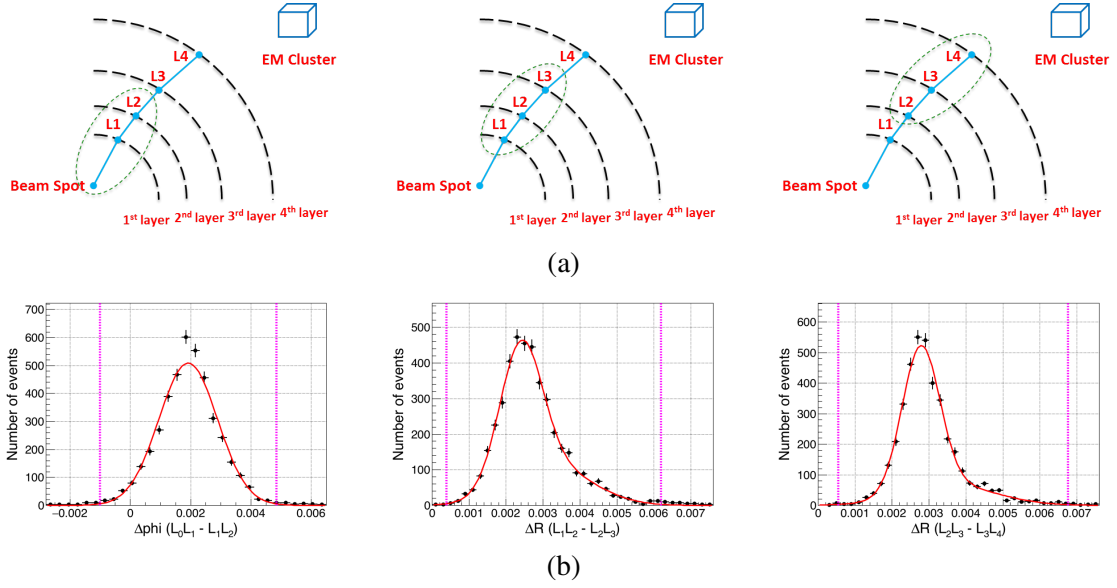


Figure 6. Standalone pattern recognition with pixel clusters: (a) top views shows all possible three aligned clusters cases including also BS. (b) Left plot shows the corresponding $\Delta\phi = \phi(L_0, L_1) - \phi(L_1, L_2)$ to the top left schema. Middle plot shows the ΔR corresponding to the top middle schema and right plot shows the ΔR corresponding to the top right schema. All the distributions include the three sigma boundary and correspond to EM transverse energy (E_T) range from 20 to 21 GeV.

Where $i, j = 1, \dots, 4$ and $i \neq j$. The pixel cluster in each layer is then selected only and only if it passes all the possible signal windows within 3 standard deviations as shown in figure 5.

3.2 The standalone pattern recognition

This second step aims to still reduce the possible remaining fake pixel clusters. To do so, we now look for all the possible three aligned clusters, with all the remaining pixel clusters in each of the 4 layers including also the beam spot. The $\Delta\phi$, $\Delta\eta$ and ΔR signal windows (figure 6), in function of EM E_T , are now defined by:

$$\begin{aligned}\Delta\eta &= \eta(L_i, L_j) - \eta(L_j, L_k) \\ \Delta\phi &= \phi(L_i, L_j) - \phi(L_j, L_k) \\ \Delta R &= \sqrt{(\Delta\eta)^2 + (\Delta\phi)^2}\end{aligned}\tag{3.3}$$

Where $i, j, k = 0, \dots, 4$ with $L_0 = BS$ and $i \neq j \neq k$. The pixel cluster must satisfy all the signal windows requirements within 3 standard deviations. The complete procedure allows achieving a good pattern recognition by giving a complete set of pixel clusters defined by a series of $\Delta\eta$, $\Delta\phi$ and ΔR signal windows. The selected clusters can then be used to perform a track fit reconstruction which is not the purpose of this present series of exercise.

4. Preliminary outcomes from feasibility studies on a L1 pixel based electron trigger

Applying the PiXTRK algorithm to the case of a L1 trigger on electrons for HL-LHC ($\langle 140 \rangle$ PU),

we obtain an overall efficiency of 93% in the central barrel and a rejection factor for fake electron of 8 for a L1 EM E_T threshold of 20 GeV. This is a first very encouraging indication of the strength of such a trigger. It means the L1 pixel trigger allows that the L1 EM E_T trigger threshold can be significantly lowered in the L1 when L1 EM objects are matched to the pixel based tracks even in an average PU of 140. This trigger would imply to be able to reconstruct the electron track from the pixel clusters, as seeded by the corresponding L1 EM trigger tower (see section 3). A series of other feasibility studies in CMS are underway for the extension in η of this trigger and for the use for b -tagging in the first level of trigger (using the L1 outer track as a seed).

5. EXERCISES

The exercises for introducing the students to a L1 pixel-based tracking trigger algorithm are made of the following four series of exercises.

- (1) In the exercise 1-1, the students are introduced to the ROOT-based software framework and the CMS pixel data format. In exercises 1-2 & 1-3 (figure 7 (a) and (b)), the students learn the CMS pixel detector geometry. In exercise 1-4, the students get to also understand the granularity of the EM calorimeter and the size in elementary cells that defines the L1 EM trigger tower (figure 7 (c) and (d)). The dimension of the L1 EM tower is instrumental for defining the "region of interest" as the L1 trigger tower size defines the dimension of the seed in this case. The last step in the first exercise is to understand the correlation between the electron as defined at the generator-level and the L1 EM cluster that indeed serves to the identification of the electron. The figure 7 (e) shows how the measured transverse energy agrees well with the electron momentum as defined at the generator-level within a given resolution.
 - Exercise 1-1 : Understanding the Ntuple data structure in the ROOT framework
 - Exercise 1-2 : Drawing the pixel geometry in the X-Y plane using pixel clusters on each pixel layer (figure 7 (a))
 - Exercise 1-3 : Drawing the pixel geometry in the R-Z plane using pixel clusters on each pixel layer and each disk (figure 7 (b))
 - Exercise 1-4 : Drawing separately the L1 EM cluster η and ϕ distributions (figure 7 (c) and (d))
 - Exercise 1-5 : Drawing the 2-dimensional plot between the generation-level electron transverse momentum (p_T) vs. the L1 EM E_T (figure 7 (e)).
- (2) The purpose of the second exercise is to match the track reconstructed with pixel clusters with the generator-level electron and with the L1 EM cluster. In the exercise 2-1, the students have to simply calculate the η and ϕ angles in cylindrical coordinates from the pixel clusters defined in cartesian coordinates (figures 8 (a) and (b)).
 Using the previously obtained η and ϕ coordinates, the $\Delta\eta$ and $\Delta\phi$ distributions defined as the difference between the η (respectively ϕ) coordinate of the pixel cluster on each layer

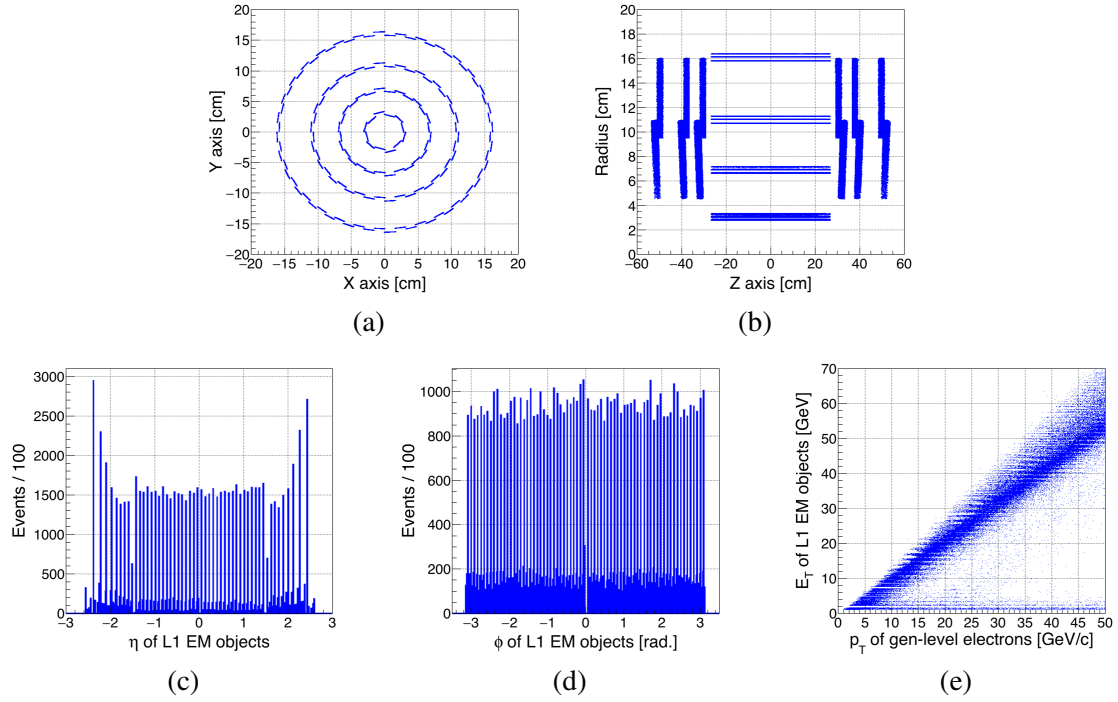


Figure 7. EXERCISE 1 results: Exercise 1-1 (a): view of pixel layers in X-Y plane; Exercise 1-2 (b): view of pixel layers and disks in R-Z plane; Exercise 1-3 (c): η distribution of L1 EM clusters; Exercise 1-4 (d): ϕ distribution of L1 EM clusters; Exercise 1-5 (e): 2-dimensional distribution of gen-level electron E_T vs. L1 EM E_T

and the η (respectively ϕ) of the generator-level electron or the η (respectively ϕ) of the L1 EM cluster are drawn in the exercises 2-2 & 2-3 (figures 8 (c) and (d)).

This step is for understanding how precisely one can determine the $\Delta\eta$ and $\Delta\phi$ signal windows using the pixel detector and the L1 EM calorimeter (figures 8 (e) and (f)).

- Exercise 2-1 : Transferring the (x,y,z) pixel cluster position to its η and ϕ cylindrical coordinates and drawing the corresponding η and ϕ distributions only in the case of the first barrel pixel layer (figures 8 (a) and (b)).
- Exercise 2-2 : Drawing the $\Delta\eta$ and $\Delta\phi$ distributions between the pixel cluster in the first barrel layer and the generator-level electron as previously defined (figures 8 (c) and (d)).
- Exercise 2-3 : Drawing the $\Delta\eta$ and $\Delta\phi$ distributions between the pixel cluster in the first barrel layer and the L1 EM cluster as previously defined (figures 8 (e) and (f)).

- (3) The goal of the third exercise is to evaluate the size of the signal windows in two cases, one based on tracks segments using only the pixel clusters (see figure 6) i.e. *standalone pixel tracking*, the other one using tracks based on pixel clusters matching with the corresponding L1 EM cluster as shown for instance in figures 4 and 5 (b) i.e. *pixel track seed by EM cluster*.

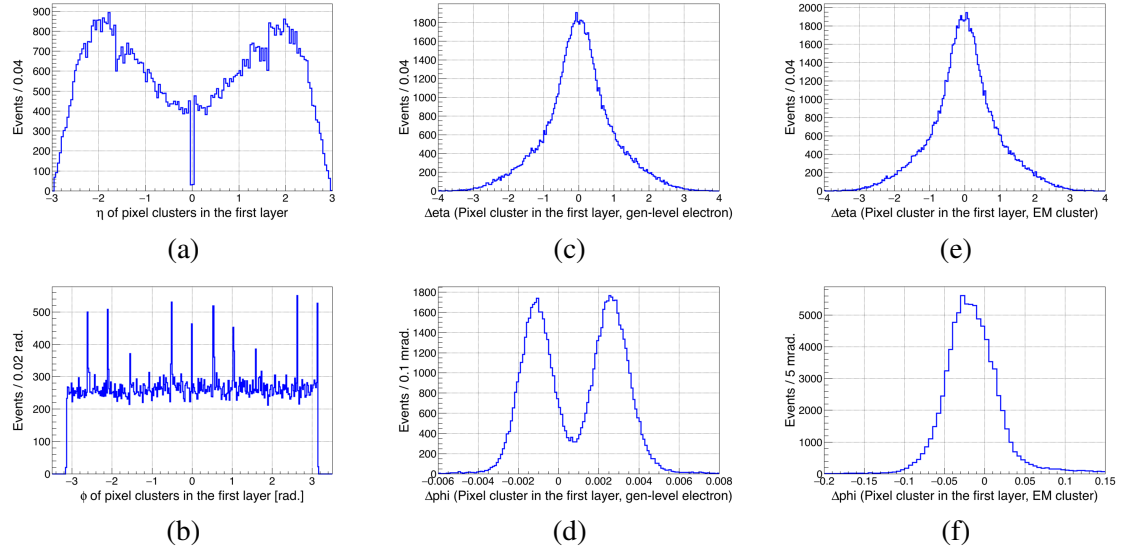


Figure 8. EXERCISE 2 results: Exercise 2-1: η (a) and ϕ (b) distributions of pixel clusters in the first pixel layer; Exercise 2-2: $\Delta\eta$ (c) and $\Delta\phi$ (d) distributions between pixel clusters in the first pixel layer and gen-level electron; Exercise 2-3: $\Delta\eta$ (e) and $\Delta\phi$ (f) distributions between pixel clusters in the first pixel layer and L1 EM cluster

The first case (pixel standalone tracking) of the third exercise consists in getting the $\Delta\eta$, $\Delta\phi$ and ΔR signal windows using the corresponding pixel clusters in the first, second and third pixel layers. To do so, the students have simply to edit the basic generic source code provided to them. This source code allows extracting from the Ntuple the needed parameters. In this case it is used to compare $\Delta\eta$, $\Delta\phi$ and ΔR angle differences between the track segment defined with the corresponding aligned clusters in the first and second layers and the track segment defined with the corresponding aligned clusters in the second and third layers for determining the corresponding η and ϕ signal windows (figure 6 (b)).

The second case (EM cluster seed case) consists in determining the $\Delta\eta$ (figure 9 (d)), $\Delta\phi$ (figure 9 (e)) and ΔR (figure 9 (f)) distributions computed as the difference in η and ϕ between the pixel track segment defined between corresponding aligned clusters in the first and fourth layers and the η and ϕ of the segment linking the origin (0,0,0) to the L1 EM cluster.

- Exercise 3-1 : Drawing the $\Delta\eta$, $\Delta\phi$ and ΔR signal windows in the case of standalone tracking pixel case (figure 9 (a), (b) and (c)).
- Exercise 3-2 : Drawing the $\Delta\eta$, $\Delta\phi$ and ΔR signal windows in the case of the pixel track seed by EM cluster (figure 9 (d), (e) and (f)).

- (4) The goal of the fourth exercise is to calculate the signal efficiency and the background rejection factor. This is based on determining all the signal windows. It means the signal windows defined both in the standalone case and the EM cluster seed case. In the standalone case, the signal windows are computed with three pixel clusters using four pixel layers (including the beam spot). In the EM cluster seed case, the signal windows are

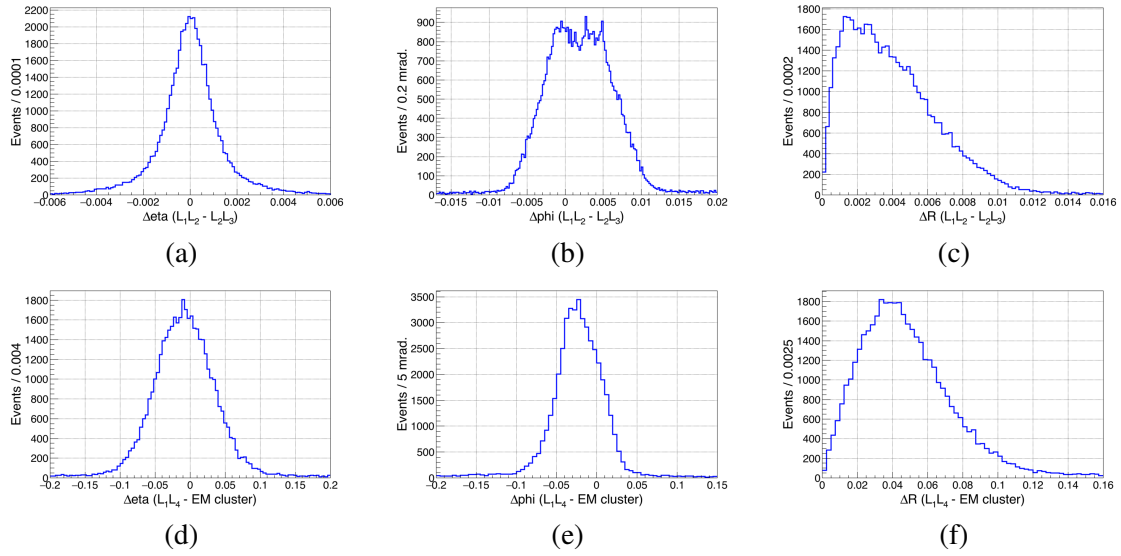


Figure 9. EXERCISE 3 results: Exercise 3-1: $\Delta\eta$ (a), $\Delta\phi$ (b) and ΔR (c) distributions between aligned clusters in the first and second layers and aligned clusters in the second and third layers; Exercise 3-2: $\Delta\eta$ (d), $\Delta\phi$ (e) and ΔR (f) distributions between colinear pixel clusters in the first and fourth layers and L1 EM cluster

computed with two pixel clusters and their matching with the corresponding EM cluster for all the possible combinations using the four pixel layers.

The electron efficiency of this trigger is defined as the ratio of the total number of events satisfying all the requirements on all the calculated signal windows to the total number of events selected by the L1 EM calorimeter trigger and matching in $\Delta R < 0.2$ with the generator-level electron (ensuring the L1 EM objects are true electrons).

The potential of an electron trigger is also determined by its capability to reject “fake electron”. The “fake electron” are objects which pass the L1 EM trigger conditions although they are not true electrons. To study “fake electron”, one use minimum bias data and apply to them the L1 EM trigger conditions to extract a “fake electron” sample. The fake electron rejection factor is then defined with this minimum bias samples as the ratio.

With this exercise, the students get to know how to distinguish a real electron candidate from a fake electron.

The background rejection factor is defined as the ratio of the total number of events that do not satisfy at least one requirement on the signal windows to the total number of events selected by the L1 EM calorimeter trigger.

In the final step, the students learn how to calculate the trigger efficiency and the fake electron rejection factor as a function of the L1 EM E_T trigger threshold.

- Exercise 4-1 : Drawing the electron trigger efficiency as a function of L1 EM E_T trigger threshold (figure 10 (a))
- Exercise 4-2 : Drawing the fake electron rejection factor as a function of L1 EM E_T trigger threshold (figure 10 (b))

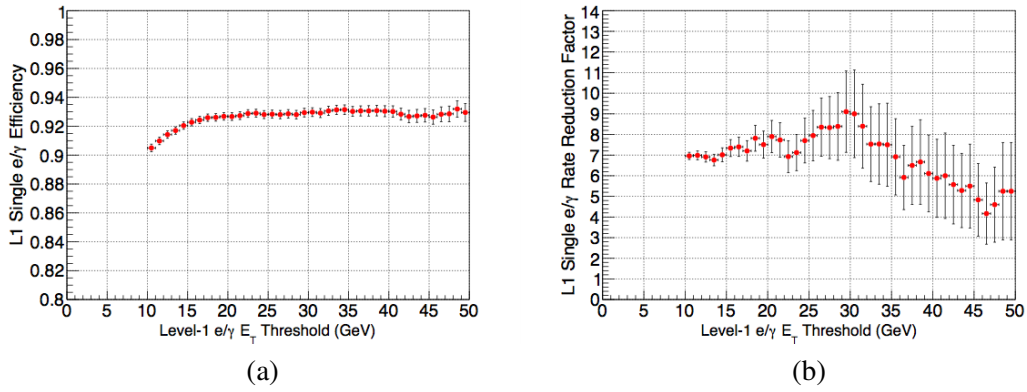


Figure 10. EXERCISE 4 results: Exercise 4-1: pixel based trigger efficiency (a) and Exercise 4-2: L1 single EM trigger rate reduction factor with pixel information (b) as a function of pseudorapidity

6. Conclusion

This series of exercises aims to introduce the students to an important topic for future HEP experiments namely the potential use of the pixel detector in the L1 trigger or the real-time tracking. It also shows the basic way to address the real-time tracking based on the pixel hits by building track segments in standalone or seed based tracking modes. This is indeed a very challenging and new tracking trigger approach especially in the harsh HL-LHC environment.

Acknowledgments

We acknowledge the support from the EU community Marie Curie International Incoming Fellowship (IIF), FP7-PEOPLE-2011-IIF, Contract No. 302103, TauKitforNewPhysics (Tau Toolkit for opening the New Physics Window at LHC and possible spin off effects). And we thank our colleagues from the CMS collaboration for providing the overall CMS simulation framework.

References

- [1] CMS Collaboration, *The CMS experiment at the CERN LHC*, JINST 3 S08004 (2008).
- [2] CMS Collaboration, *CMS Technical Design Report for the Pixel Detector Upgrade*, CERN-LHCC-2012-016 (2012).
- [3] CMS Collaboration, *The TriDAS project, technical design report. Volume 2: Data acquisition and high-level trigger technical design report*, CERN-LHCC-2002-026, <http://cds.cern.ch/record/578006>.
- [4] 2nd International Summer School on: *INtelligent Signal Processing for FrontIER Research and Industry*, held in Paris July 14-25, 2014, <http://infieri2014summerschool.in2p3.fr>.
- [5] CMS Collaboration, *The pixel detector for the CMS phase-II upgrade*, JINST 10 C04019 (2015).
- [6] RD53 Collaboration, *RD53 Collaboration Proposal: Development of pixel readout integrated circuits for extreme rate and radiation*, CERN-LHCC-2013-008 (2013).
- [7] CMS Collaboration, *Technical Proposal for the Phase 2 Upgrade of the CMS Detector*, CERN-LHCC-2015-010 (2015), <http://cds.cern.ch/record/2020886>